J Therm Spray Tech (2020) 29:1958–1967
https://doi.org/10.1007/s11666-020-01116-4

PEER REVIEWED

Effect of the Corrosion of Seal Coatings Used in Aero Engines on Their High-Speed Wear Behaviour

Jiaping Zhang[1,2] · Weihai Xue[1] · Deli Duan[1] · Shengli Jiang[1] · Jia Song[2] · Siyang Gao[1] · Shu Li[1]

Submitted: 8 January 2020 / in revised form: 12 October 2020 / Accepted: 19 October 2020 / Published online: 4 November 2020

Abstract As the number of aircraft that park in ocean environments increases, the corrosion of coatings used in their engines becomes inevitable. Previous studies have focussed on the abradability of as-sprayed seal coatings in high-speed rubbing tests with a blade. This study deals with the investigation of the effect of corrosion on the abradability of seal coatings. It uses metallographic analysis and hardness, bonding strength and high-speed rubbing tests conducted on as-sprayed and corroded Al-hBN coatings. The results have shown the appearance of additional pores in the corroded coatings and a decrease in the coating mechanical properties. Compared with the as-sprayed coatings, the corroded coatings caused an increase in blade wear and severe overheating of the blade tip during the high-speed rubbing test when the rubbing speed and single-pass depth were high. The unfavourable thermal properties of the corroded coatings were considered as the probable reason for these results.

Keywords abradable seal coating · high-speed rubbing · salt spray corrosion · thermal property

✉ Weihai Xue
whxue@imr.ac.cn

✉ Deli Duan
duandl@imr.ac.cn

[1] Institute of Metal Research, Chinese Academy of Sciences, Shenyang 110043, China

[2] AECC Shenyang Liming Aero-Engine Co., Ltd., Shenyang 110043, China

Introduction

Abradable seal coatings are sprayed onto aero-engine cases, thus forming a friction pair with the rotating blade. When the clearance between the case and the blade becomes smaller due to thermal expansion or elongation of the high-speed rotating blade, the blade will first rub the coating. Rubbing results in a wear scar that fits the blade outline in the coating; thus, the clearance can be maintained to the smallest scale (Ref 1–4). Based on the working principle of the seal coating, abradability is the most important property of the seal coating. Abradability means that the rubbing between the seal coating and the rotating blade results in as little damage as possible to the blade, as minimal adhesion of the coating material to the blade as possible, and a smooth coating wear scar.

Al-hBN coatings are widely used as a seal coating in aero-engine compressors. Many studies have been conducted to study the abradability of such coatings using high-speed rubbing rigs. Stringer (Ref 5) focused on the influences of linear speed and single-pass depth on high-speed wear behaviour, and found that the adhesion of coating material to the blade aggravated when the single-pass depth was low. Fois (Ref 6) conducted further research on adhesion behaviour of coating material to the blade using a stroboscopic imaging technique and found that the adhesion of coating material to the blade could be divided into three stages, namely, beginning, stabilisation and peel off, followed by re-adhesion. Xue (Ref 7) conducted high-speed rubbing tests of the Al-hBN coating at different linear speeds and single-pass depths. Significant adhesion of coating material to the blade was found at the combination of high linear speed and low single-pass depth. The adhesion material was composed of metal-phase aluminium. Gao (Ref 8) studied the effect of the thermal

physical properties of the coating–blade system on high-speed rubbing behaviour. The test results indicated that the different temperature increase rates of the blade and the coating were due to the frictional heat conduction that decides the wear behaviour.

With the increasing number of aero engines, such as shipboard aircraft, that park in ocean environments, the corrosion behaviour of seal coatings has elicited considerable attention. Especially for military aircraft, whose parking time accounts for nearly 90% of their entire working life, coating corrosion during parking cannot be ignored. Xu (Ref 9) studied the corrosion behaviour of the 75Ni/25graphite abradable coating and Ni–Al bonding coatings with different Al content. The experimental results showed that the corrosion resistance of the Ni–Al coatings decreased with increasing Al content. Lei (Ref 10) researched the corrosion mechanism of an aluminium–boron nitride (Al-BN) abradable coating system (with a NiAl bond layer and 0Cr17Ni4-Cu4Nb substrate) in chloride solution. Zhang (Ref 11) conducted spray tests on a novel NiTi/BN composite abradable coating and found that the NiTi/BN coating showed superior corrosion resistance over the Ni/BN and Ni/graphite coatings.

On the basis of the actual working process (i.e. parking–flying–parking) of aero engines in ocean environments, the seal coating rubbed by the rotating blade becomes corroded. However, very limited research on the high-speed rubbing behaviour of the corroded coating has been conducted. The applicability of the abradability evaluation of coatings under as-sprayed condition for seal coatings in ocean environments, and the influence mechanism of corrosion on abradability, needs investigating.

In this study, high-speed rubbing tests are conducted on coatings that underwent salt-sprayed and atmospheric exposure corrosion. Compared with the high-speed rubbing tests on as-sprayed coatings, the effects of corrosion on the abradability of an Al-hBN coating are studied. This research contributes to the application of Al-hBN coatings in an ocean environment and to safe aero-engine operation.

Experimental and Materials

High-Speed Rubbing Test Rig

The rubbing between the seal coating and the blade is characterised by high-speed, high-temperature and interrupted contact. General friction and wear testing machines cannot meet the test requirements. Therefore, a frequently used abradability evaluation testing method is to build a high-speed, high-temperature rubbing test rig that can simulate the working conditions of seal coatings. All the tests in this study were conducted with a high-speed rubbing test rig built by AECC Shenyang Liming Aeroengine and the AVIC Beijing Precision Engineering Institute for Aircraft Industry. The test rig is shown in Fig. 1.

The working principle of the test rig is presented in Fig. 2. The blade sample is inserted into a metal disc that is driven by a high-speed motorised spindle. Driven by the spindle, the blade sample rotates and simulates the rotor motion in an aero engine. With the help of a sliding table, the coating sample is stepped forward to the rotating blade sample at a predefined speed and incursion depth. As soon as the coating contacts the rotating blade, rubbing begins. The normal and tangential forces generated during rubbing are recorded by measuring equipment.

Materials

To improve the simulation of the rubbing condition between the seal coating and the blade, the coating and blade sample materials used in this experiment must be consistent with the actual engine. The coating sample was an Al-hBN coating, which was sprayed on a

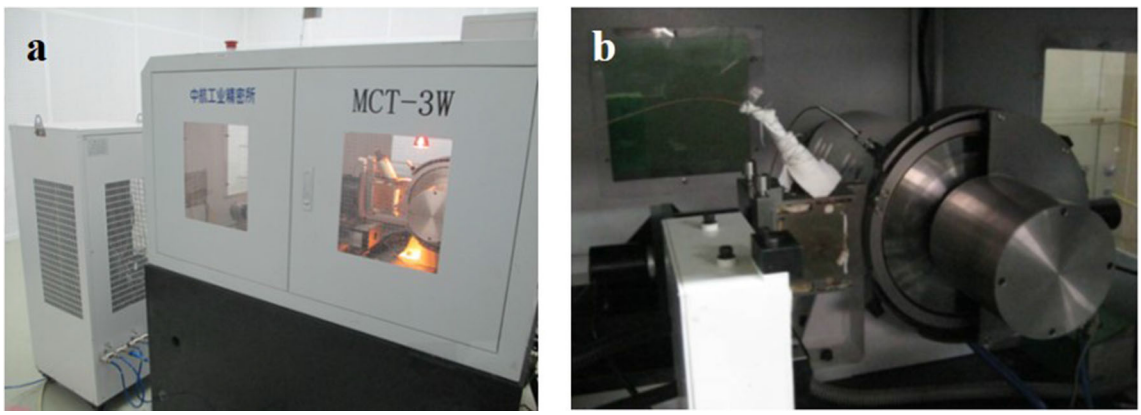

Fig. 1 (a) The high-speed rubbing test rig and (b) details of the rubbing region

0Cr17Ni4Cu4Nb stainless-steel substrate using a METCO 9MC plasma spraying equipment. The substrate size was 20 × 40 × 2 mm. Before spraying, a NiAl bonding layer was deposited on the substrate to improve the bonding strength between the coating and the substrate. The final thickness of the NiAl bonding layer was 0.1–0.2 mm, and the final thickness of the Al/BN surface layer was approximately 2.5 mm. The composition and mass percent of the coating powder was 75% Al, 20% BN and 5% Na_2SiO_3. The micro-morphology of the coating powder is shown in Fig. 3(a). The main spraying process parameters were as follows: argon flow rate of 2.5 m^3/h, hydrogen flow rate of 0.2 m^3/h, powder delivery rate of 45 g/min and spraying distance of 130 mm. The section microstructure of the as-sprayed Al-hBN coating is shown in Fig. 3(b); the coating was mainly composed of metallic phase Al, solid lubrication phase BN and pores.

The blade sample was made of a TA11 titanium alloy and processed by electrosparking into the required installation shape and size. The final rubbing surface with the coating was a rectangle of 20 × 2 mm.

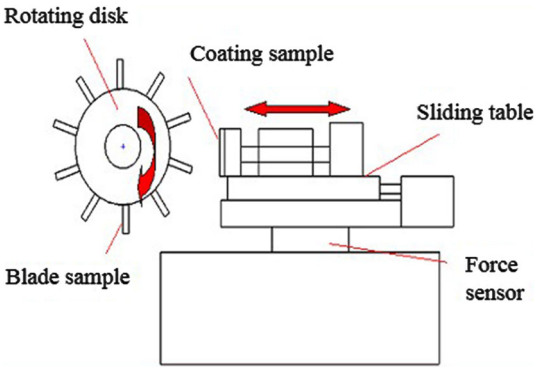

Fig. 2 Schematic of the high-speed rubbing rig

Testing Method

On the basis of the investigation of the engine type, working environment and service conditions, the general linear speed of the rotor was 250–350 m/s, and the coating thickness was decreased by 200–500 μm during one maintenance period. In this study, the linear speed of the high-speed rubbing test was set as 350 m/s, the feed speed was 13 μm/s, and the feed depth was 0.5 mm. Salt spray corrosion experiment has been used to simulate the corrosion environment of an aero engine parked in an ocean environment. The salt-spray corrosion experiments of the Al-hBN seal coatings were conducted in a neutral salt fog atmosphere using a DCTC1200P salt spray testing machine according to the standard ASTM B117. There are two exposure durations, 48 h and 96 h. The salt spray solution was 5 wt% NaCl, and the sample put angle was 30°. Atmospheric corrosion experiments were simultaneously conducted at the Qingdao China Marine Station (C4, ISO9223) to simulate the actual marine atmospheric corrosion that Al-hBN seal coatings undergo when the engine is parked. The test duration was 1046 h. To eliminate the effects of corrosion on the interface, the interface area between the coating and the substrate was packaged with epoxy resin.

An electronic balance with a precision of 0.1 mg was used to weigh the coating and blade samples before and after the high-speed rubbing test, and a Vernier calliper with a precision of 0.01 mm was used to measure the blade height variation. All the coating samples for metallographical and micro-morphology analysis were prepared through vacuum resin infusion. Then, the coating samples embedded in resin were ground with sand paper and polished with polishing paste. An FEI INSPECT F50 scanning electron microscope (SEM) was used to observe the wear scars on the blade and the coating, and the element composition of the wear scar surface was analysed using an EDAX spectrometer. A Nikon D3100 digital camera was

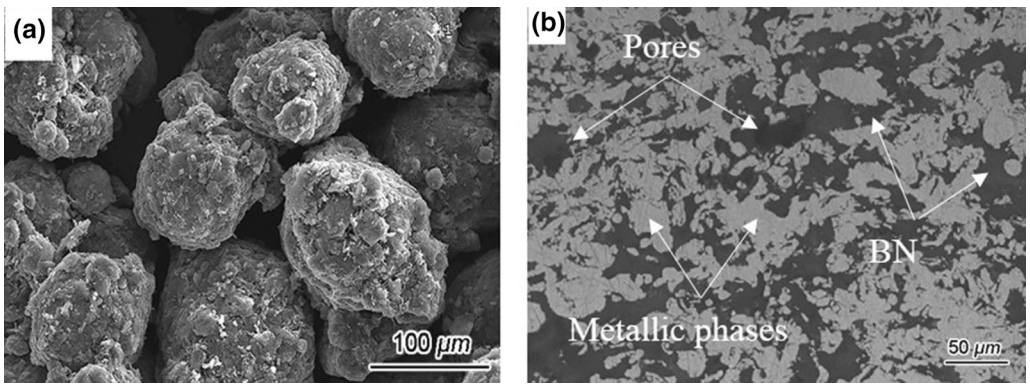

Fig. 3 Micro-morphology of the coating powder (a) and metallography image of the coating section (b)

used to observe the macroscopic morphology of wear scars on the blade and the coating. The surface hardness of the coating was measured via the surface Brinell hardness test method; the indentation load was 612.9 N, and the load holding time was 10–15 s. The tensile bonding strength of the coating was measured on the basis of the ASTM C633-01 standard.

Results and Analysis

Morphologies of the Corroded Coating

The surfaces of the corroded coatings that underwent salt spray and atmospheric corrosion are shown in Fig. 4. According to the x-ray defraction (XRD) detection result of the corroded coating surface (Fig. 5) and the neutral salt spray corrosion research results on the aluminium alloy (Ref 12), colloidal $Al(OH)_3$/AlO(OH) and oxide of aluminium covered the coating surface after 96 h of salt spraying. White particles on the coating surface suffered atmospheric corrosion probably due to the air-seasoning of the colloidal $Al(OH)_3$.

SEM observation and energy-dispersive x-ray spectroscopy (EDS) analysis were conducted on the corroded coating surface (the corroded coating samples were ground with sand paper and polished). As presented in Fig. 6, the metal phase in the coating experienced corrosion and resulted in some large and deep pores. As a result of the corrosion, gaps between the metal and lubrication phases appeared. The EDS results indicated that the corroded coating metal phase was mainly composed of aluminium and oxygen. In the other area, elements, such as Na, Cl and Si, were identified, indicating that many corrosion products were produced.

Influences of Corrosion on the Coating Structure and Properties

The cross-sectional microstructure of the as-sprayed and corroded coatings are shown in Fig. 7. The phase contents were determined using phase analysis software. In the as-sprayed coating, the ratio of metal to nonmetallic phase was 63 to 37. In the corroded coating, this ratio was 40 to 60. Figure 7 clearly shows that the increase in nonmetallic phase (composed of pores filled by resin and boron nitride phase) resulted from the pore increase. Also, there are some corrosion products found in the section image (Fig. 7b).

Surface Brinell hardness tests were conducted on the as-sprayed and corroded coatings. The average indentation diameter of the as-sprayed coating was 2.61 mm. After undergoing a 96-h salt spray test, the average indentation diameter was 2.68 mm. The corresponding Brinell hardness was 10.8 HB (SD 0.05) and 10.2 HB (SD 0.21), indicating that the hardness of the corroded coating decreased by approximately 6% in comparison with the as-sprayed coating.

The tensile bonding strengths of the as-sprayed coatings and coatings that underwent different salt-spray corrosion durations were tested according to the Chinese industry standard, HB20035-2013. Resin glue (FM-1000) was used to bind the coating surface to the holder. A tensile testing machine (AG-250KNE; INSTRON, USA) was used to test the bonding strength, and the extension rate was 1 mm/min. The average bonding strength of the as-sprayed coating was 9.2 $\pm$ 1.46 MPa. After testing in salt spray for 48 h, the average bonding strength of the coating decreased to 4.4 $\pm$ 1.08 MPa; for 96 h, and the average bonding strength decreased to 2.69 MPa. Observations of the tested coating samples (Fig. 8a) showed that the fracture occurred only in the surface layer of the coating that underwent 48 h of salt spray, so only the binding layer was exposed. When the coating experienced 96 h of salt spray (Fig. 8b), fractures at the interface between the substrate and bonding layer were observed, so the corroded substrate was exposed. Corrosion had important effects on the coating bonding strength.

High-Speed Rubbing Test Results of the As-Sprayed and Corroded Coatings

High-speed rubbing tests were conducted with the as-sprayed coating and the corroded coating to explore the

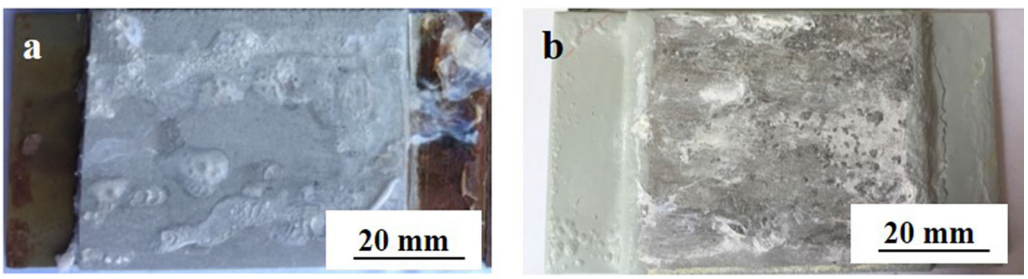

Fig. 4 Surface morphologies of the corroded coatings resulting from (a) salt spray (96 h) and (b) atmospheric corrosion (1046 h)

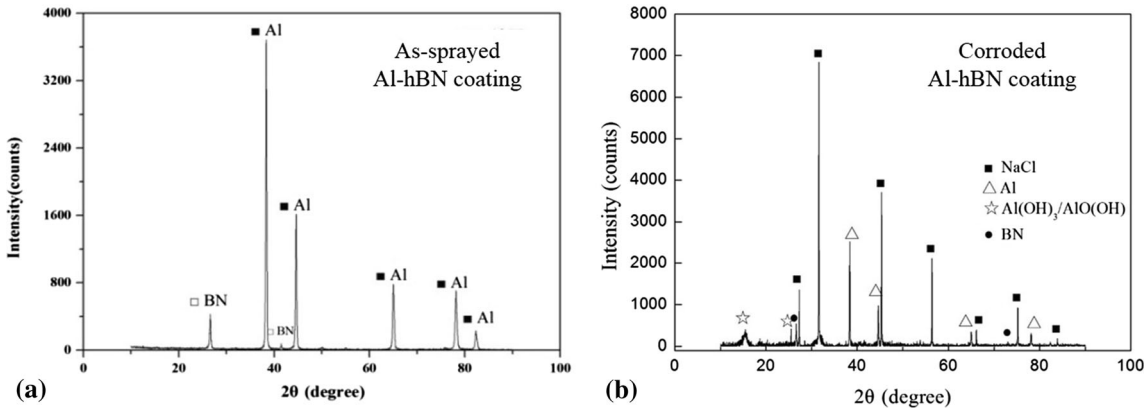

Fig. 5 XRD detection results of the as-sprayed coating (a) and corroded coating (b)

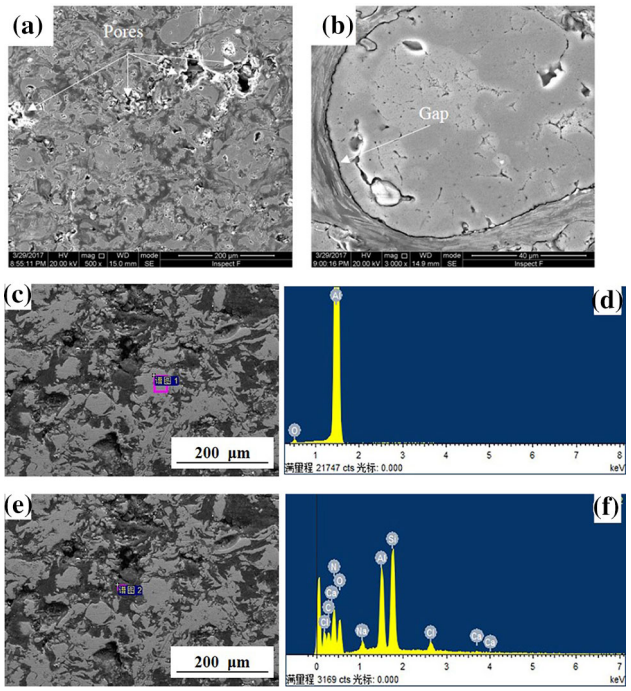

Fig. 6 (a, b) SEM morphologies of the corroded Al/BN coating surfaces and EDS results in the ©) (d) metal and (e, f) nonmetallic phases

effect of corrosion on the abradability of the Al-hBN seal coating. The test parameters are shown in Table 1. The coating underwent atmospheric corrosion due to the long exposure time (1046 h); the high-speed rubbing test was only performed at a linear speed of 300 m/s and single-pass depth of 0.036 μm to prevent the entire coating from peeling off.

The test results are shown in Table 2. A positive value indicates height or weight loss, while a negative value meant height or weight gain. Blade height gain does not always come with blade weight gain. A similar situation was found with blade height loss because the adhesion of coating material to the blade and blade wear could occur during a single rubbing test.

Test 1 shows that the obtained wear results from the salt-spray tests and atmospheric corrosion tests were similar, indicating that the salt-spray test could be used as an accelerated test instead of atmospheric corrosion. Thus, the following analysis of the rubbing behaviour at 300 m/s used the test results of the salt-spayed coating.

A comparison of the test results with the as-sprayed and corroded coatings revealed that both coatings adhered to the blades when rubbed at 300 m/s. The blade height increase of the blade rubbed against the as-sprayed coating was larger than that of the blade rubbed against the corroded coating. However, the blade weight gain of the blade rubbed against the as-sprayed coating was less than that of the blade rubbed against the corroded coating. The possible reason for this result is the uneven adhesion of coating material to the blade. At a rubbing rate of 350 m/s, aggravated blade wear occurred when the blade was rubbed against the corroded coating at both single-pass depths.

Blade Wear Scar Morphologies

The surface (top) and cross-section (bottom) images of the blade tips rubbed against as- and salt-sprayed coatings are shown in Fig. 9. When the linear speed was 300 m/s (Fig. 9a, b), both coatings adhered to the blades. However, the blade tip rubbing against the as-sprayed coating received considerable adhesion of coating material to the blade, which was highly uneven. Thus, the resulted blade height variation was large with a small blade weight gain (Table 2).

At a rubbing rate of 350 m/s, when the single-pass depth was low (Fig. 9c, d), adhesion of coating material to the blade and overheating regions was found on the blade tip rubbed against the as-sprayed coating. When the blade rubbed against the corroded coating, no adhesion of coating material to the blade was found on the blade tip and

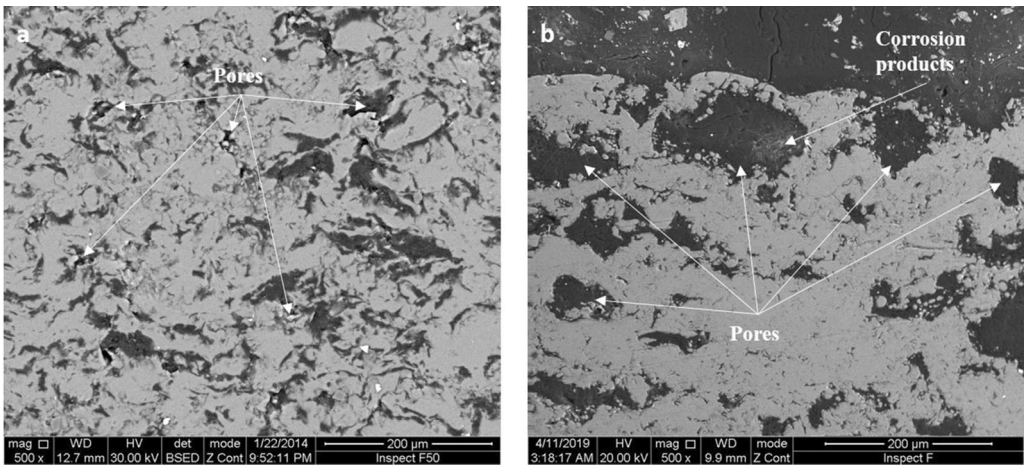

Fig. 7 SEM images of the as-sprayed coating section (a) and corroded coating section (b)

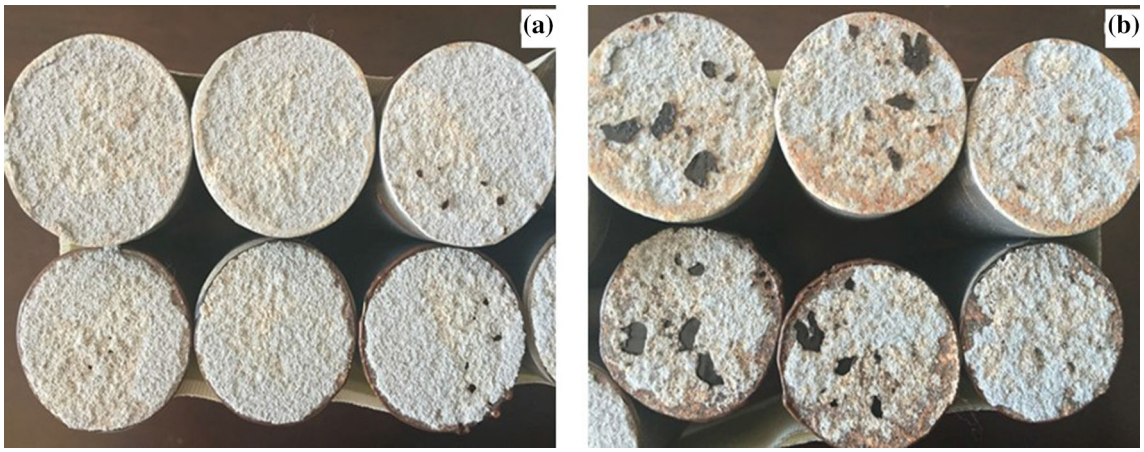

Fig. 8 Fracture appearances of the tensile bonding strength test of the coating corroded for 48 h (a) and 96 h (b)

Table 1 High-speed rubbing test parameters

Test no.	Single-pass depth, µm	Linear speed, m/s	Incursion speed, µm/s	Incursion depth, µm
1	0.036	300	12	500
2	0.036	350	15	500
3	0.072	350	30	500

Table 2 High-speed rubbing test results

Test no.	Coating condition	Blade height variation, mm	Blade weight loss, mg
1	As-sprayed	−0.465	−7
	Salt-sprayed	−0.104	−14
	Marine atmosphere	−0.04	−9.1
2	As-sprayed	0.07	−10
	Salt-sprayed	−0.192	10
3	As-sprayed	−0.04	10
	Salt-sprayed	0.04	20

furrows, of which some with considerable depths were observed. When the single-pass depth was high (Fig. 9e, f), the blade tip rubbing against the as-sprayed coating underwent adhesion of the coating material to the blade and a small overheating area. However, rubbing against the corroded coating resulted in a large overheating area, as

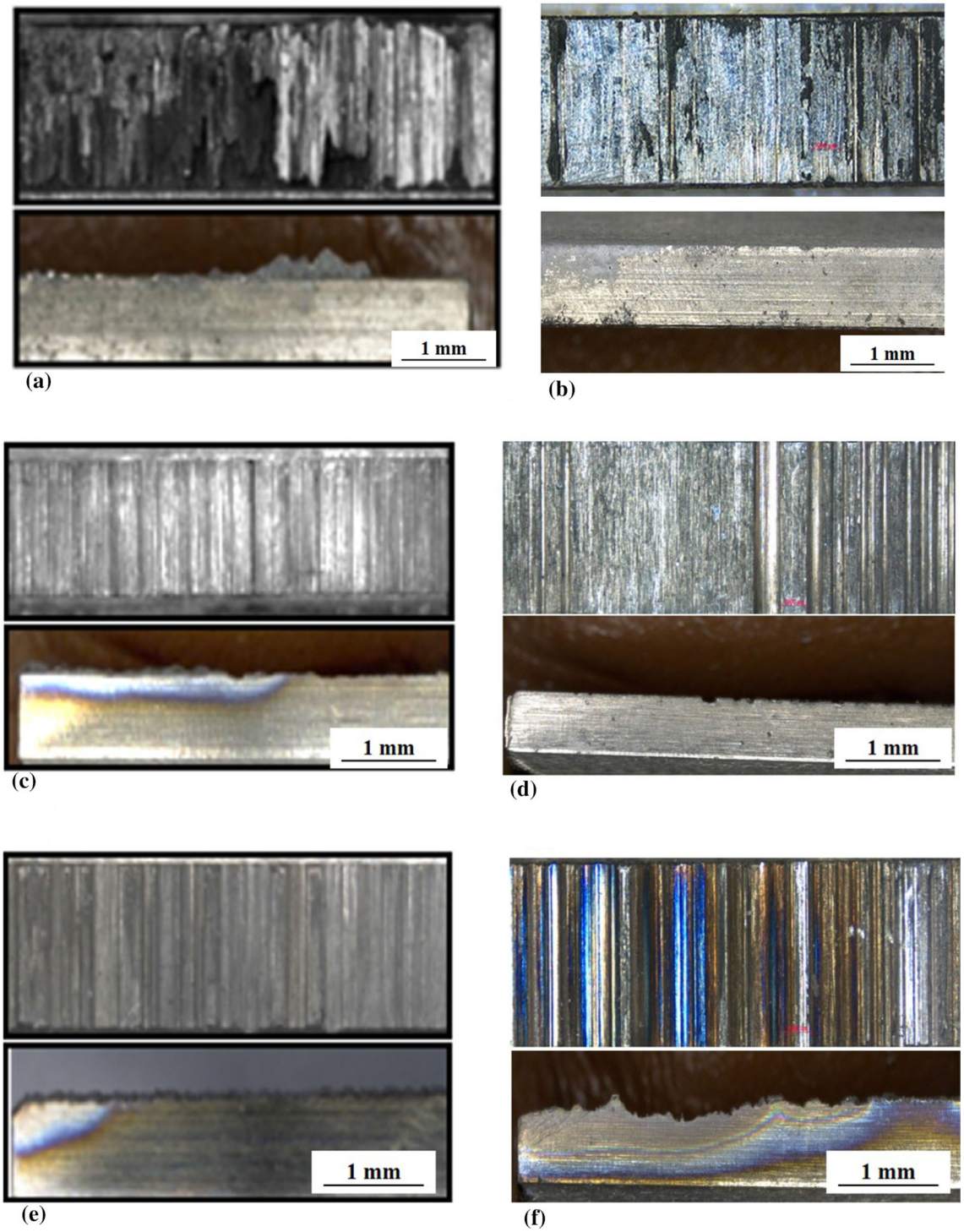

Fig. 9 Surface and cross-section morphologies of the blade tip rubbed against as-sprayed (a) and corroded coatings (b) from Test 1, as-sprayed ©) and corroded coatings (d) from Test 2, and as-sprayed (e) and corroded coatings (f) from Test 3

demonstrated by the colour change from oxidation. Many deep furrows were observed on the blade tip.

The micro-morphologies of the rubbed blade tip section are shown in Figs. 10 and 11. Rubbing against the as-sprayed coating resulted in a lamellar coating transfer layer on the blade tip and cracks in the layer. This means that adhesion of coating material to the blade could fracture and re-adhere during rubbing.

The cross-sectional microstructure of the different positions at the blade tip rubbed against the corroded

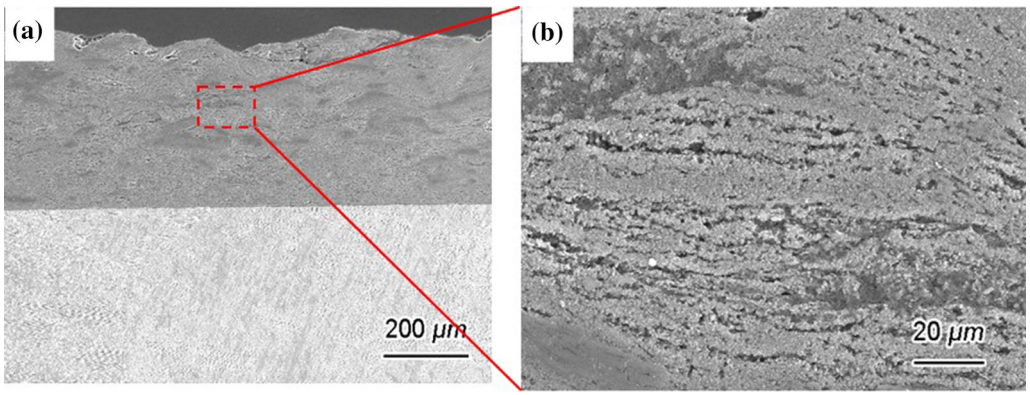

Fig. 10 Blade tip section micro-morphology: (a) low magnification, (b) magnification of the rectangular region in (a) rubbed against the as-sprayed coating at 350 m/s, 0.072 μm

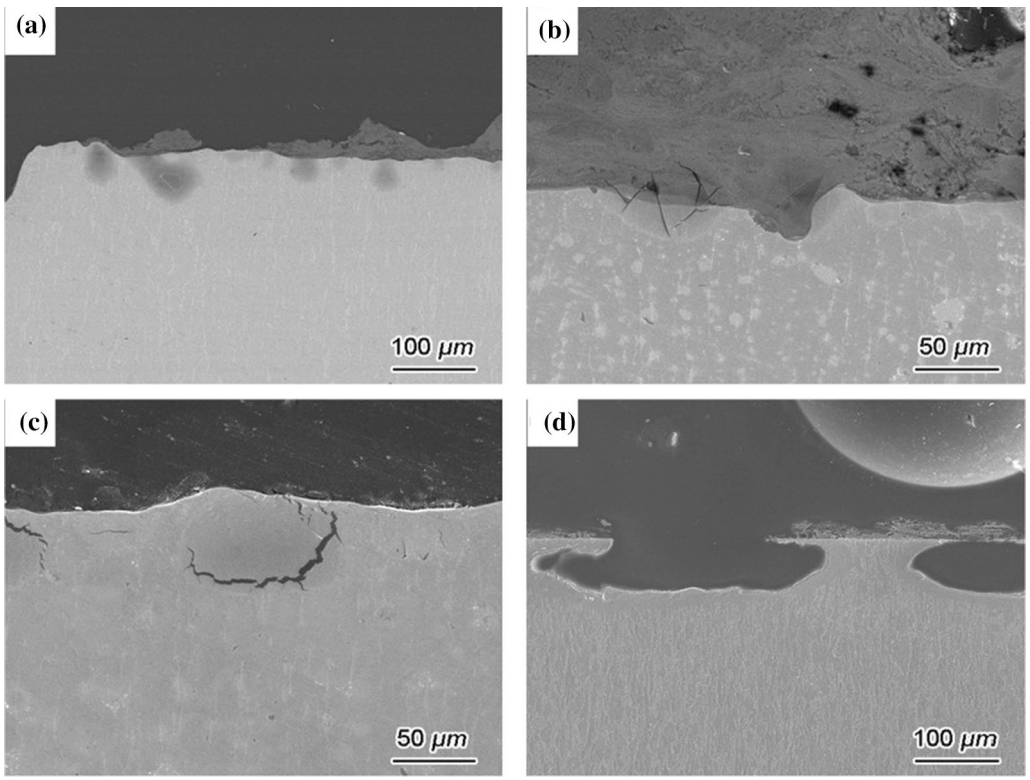

Fig. 11 Blade tip section micro-morphology rubbed against the corroded coating at 350 m/s 0.072: (a) uneven coating adhesions, (b) cracks generated in the coating adhesion, ©) cracks generated on the rubbing interface, and (d) furrows resulted from the rubbing

coating at 350 m/s 0.072 μm are presented in Fig. 11. Owing to the uneven adhesion of coating material to the blade during rubbing, the rubbing intensities on the different areas of the blade tip were different. As a result, different blade wear conditions could be observed on the different positions of the rubbed blade tip. In Fig. 11(a), dark and almost perfectly circular spots corresponding to the adhesion of coating material to the blade positions can be seen. The spots are thought to be produced by overheating from the frictional heat of high-speed rubbing. Many cracks were generated by the combined action of rubbing and thermal shock during the rub. The cracks could be generated in the adhesion of coating material to the blade (Fig. 11b) or on the rubbing interface (Fig. 11c), and propagated along the edge of the overheating region. Material loss could occur when the cracks reached the surface. As shown in Fig. 11(d), furrows were generated.

On the basis of the surface and section morphology observations of the rubbed blades, overheating and aggravated blade wear were apt to occur when the blades rubbed against the corroded coating. Adhesion and abrasive and oxidation wear were the major wear mechanisms.

Influences of Corrosion on High-Speed Rubbing Behaviour

Based on the weight variation and wear scar morphologies of the rubbed blade, aggravated blade wear and a large overheating area occurred when the blade rubbed against the corroded coating at a linear speed of 350 m/s. Thus, the corrosion had a negative effect on coating abradability.

The Al/BN coating easily corroded owing to its porous and multilayer structure. When the coating was placed in a corrosive environment, pitting corrosion could occur on the metal phase aluminium. After corrosion, the metal phase content decreased, whereas the porosity increased. These results indicated that deteriorative mechanical properties were already proven by the hardness and bonding strength tests. In addition, the single-pass pendulum scratch test of the corroded coating revealed that the energy consumed when rubbing corroded coatings decreased with the salt-spray duration (Ref 13). The single-pass pendulum scratch test had a similar rubbing action with the high-speed rubbing test, except that the scratch speed was much lower.

Corrosion made the coating weak in terms of mechanical property, and the weaker coating was easily scratched during the single-pass pendulum scratch test. However, when the rubbing speed was as high as 350 m/s, the weaker coating caused aggravated wear and overheating to the blade. Some other changed properties of the corroded coating might have influenced the high-speed rubbing behaviour.

Many published studies on the high-speed rubbing test of seal coatings and blade friction pairs have found that the thermal–physical property of the seal coating was a key factor in high-speed wear behaviour. For example, Marscher predicted that thermal effects seemed to predominate during high-speed rubbing, and that the blade tip should preferentially wear a seal-coating material when the blade tip had high conductivity with a low thermal expansion coefficient (Ref 14). Based on the study of Fois, an increased number of boundaries between the metal and the hBN phases hindered the heat flow, leading to a concentration of surface heat (Ref 15). Another study also found that high mechanical strength did not mean a lack of blade wear, and the thermal properties of the different materials blades were identified as the major reason for the different wear behaviour (Ref 16). On the basis of Archard theory (Ref 17), the average contacting surface temperate could be calculated by the following equation:

$$\theta = \frac{2qt^{\frac{1}{2}}}{(\pi K \rho c)^{\frac{1}{2}}}, \quad \text{(Eq 1)}$$

where q is the heat flux, t is the contact time, ρ and c are the density and thermal capacity of the stationary body, respectively, and K is the thermal conductivity of the stationary body (Ref 17).

In a high-speed rubbing test, the seal coating could be taken as the stationary body, and the rubbing surface temperature increased with the decrease in the coating density and thermal conductivity. As shown in the previous paragraph, the metal phase content decreased in the corroded coating, and additional pores emerged, inevitably decreasing the coating density. Moreover, additional pores resulted in extra boundaries that could hinder heat flow, and the pores inherently decreased the thermal conductivity. Thus, the thermal conductivity and density of a corroded coating were smaller than those of the as-sprayed coating, resulting in a high temperature during the high-speed rubbing. Blade wear occurred because the mechanical strength of the titanium alloy decreased quickly with the temperature (Ref 18, 19). Combined with the severer thermal shock effect, cracks (Fig. 11) were generated in the blade tip rubbed against the corroded coating.

A high temperature in the test with a corroded coating was indirectly observed. Almost no sparkle was observed by the naked eye during the rubbing with the as-sprayed coating. However, an intense sparkle was observed during the corroded coating test.

Conclusions

High-speed rubbing tests were conducted on as-sprayed and corroded Al-hBN coatings to study the influences of corrosion on the high-speed rubbing behaviour of an Al-hBN seal coating. After corrosion, additional pores and fewer metal phases were found in the corroded coating section. The hardness and bonding strength were decreased by corrosion. However, the corroded coating resulted in aggravated blade wear and a large overheating area when rubbed at a high linear speed and large single-pass depth. Decreased coating thermal conductivity and increased interfaces, which could become heat flow obstructions, were believed to be responsible for the above results.

Acknowledgment This paper was supported by the open fund of the Shenyang Key Laboratory of Aero-engine Material Tribology (SKLAMT201805) and the Strategic Priority Research Program of the Chinese Academy of Sciences (XDC04040400).

References

1. R.E. Chupp, R.C. hendricks, S.B. Lattime, and B.M. Steinetz, Sealing in Turbomachine. NASS/TM-2006-214341, 2006
2. R.C. Bill and L.P. Ludwig, Wear of Seal Materials Used in Aircraft Propulsion Systems, *Wear*, 1980, **59**(1), p 165-189
3. L.T. Shiembob, Development of Abradable Gas Path Seals. *NASA Contract. Rep., CR-134689*, 1974

4. L.P. Ludwig and R.C. Bill, Gas Path Sealing in Turbine Engines, *Tribol. Trans.*, 1980, **23**(1), p 1-22
5. J. Stringer and M.B. Marshall, High Speed Wear Testing of an Abradable Coating, *Wear*, 2012, **294–295**, p 257-263
6. N. Fois, J. Stringer, and M.B. Marshall, Adhesive Transfer in Aero-engine Abradable Linings Contact, *Wear*, 2013, **304**(1–2), p 202-210
7. W.H. Xue, S.Y. Gao, D.L. Duan, Y. Liu, and S. Li, Material Transfer Behaviour Between a Ti_6Al_4V Blade and an Aluminium Hexagonal Boron Nitride Abradable Coating During High-Speed Rubbing, *Wear*, 2015, **322–323**, p 76-90
8. S.Y. Gao, W.H. Xue, D.L. Duan, and S. Li, Tribological Behaviors of Turbofan Seal Couples from Friction Heat Perspective Under High-Speed Rubbing Condition, *Friction*, 2016, **4**(2), p 176-190
9. C.G. Xu, L.Z. Du, B. Yang, and W.G. Zhang, The Effect of Al Content on the Galvanic Corrosion Behaviour of Coupled Ni/Graphite and Ni–Al Coatings, *Corros. Sci.*, 2011, **53**(6), p 2066-2074
10. B. Lei, M. Li, Z.X. Zhao, L. Wang, Y. Li, and F.H. Wang, Corrosion Mechanism of an Al-BN Abradable Seal Coating System in Chloride Solution, *Corros. Sci.*, 2014, **79**, p 198-205
11. F. Zhang, C.G. Xu, H. Lan, C.B. Huang, Y. Zhou, L.Z. Du, and W.G. Zhang, Corrosion Behavior of an Abradable Seal Coating System, *J. Therm. Spray Technol.*, 2014, **23**(6), p 1019-1028
12. L. Li and X. Su, Corrosion Behavior of Aluminum Alloy 1050A During Cyclic Wet-Dry Immersion Test in Simulated Marine Atmospheric Enviroment, *Corros. Sci. Prot. Technol.*, 2014, **04**, p 367-386 ((in Chinese))
13. B. Lei, S.N. Hu, Z.H. Wang, Y. Li, and F.H. Wang, Corrosion-Detection and Assessment Methods for Abradable Sealing Coatings, *Corros. Sci. Prot. Technol.*, 2017, **06**, p 651-656 ((in Chinese))
14. D.M. William, A Phenomenological Model of Abradable Wear in High Performance Turbomachinery, *Wear*, 1980, **59**(1), p 191-211
15. N. Fois, M. Watson, and M. Marshall, The Influence of Material Properties on the Wear of Abradable Materials, in *Proceedings of the Institution of Mechanical Engineers. Part J, Journal of Engineering Tribology*, 2016
16. W.H. Xue, S.Y. Gao, D.L. Duan, J.P. Zhang, Y. Liu, and S. Li, Effects of Blade Material Characteristics on the High-Speed Rubbing Behavior Between Al-hBN Abradable Seal Coatings and Blades, *Wear*, 2018, **410–411**, p 25-33
17. J.F. Archard, The Temperature of Rubbing Surfaces, *Wear*, 1959, **2**(6), p 438-455
18. J. Porntadawit, V. Uthaisangsuk, and P. Choungthong, Modeling of Flow Behavior of Ti–6Al–4V Alloy at Elevated Temperatures, *Mater. Sci. Eng. A-Struct. Mater. Prop. Microstruct. Process.*, 2014, **599**, p 212-222
19. R. Ding, Z.X. Guo, and A. Wilson, Microstructural Evolution of a Ti–6Al–4V Alloy During Thermomechanical Processing, *Mater. Sci. Eng. A-Struct. Mater. Prop. Microstruct. Process.*, 2002, **327**(2), p 233-245